FLOW ANALYSIS OF A FUNNEL-STYLE SALMON EXCLUDER

Karsten BREDDERMANN[1], Mike STONE[2], Noëlle YOCHUM[3]
[1]University of Rostock, Ocean Engineering, Department of Mechanical Engineering and Marine Technology, 2, Justus-von-Liebig-Weg, Rostock, 18059, Germany
[2]Fury Group, Inc. 4005 20th Ave W #207, Seattle, WA 98199, United States of America
[3]National Oceanic and Atmospheric Administration, Alaska Fisheries Science Center, 7600 Sand Point Way NE, Seattle, WA 98115, United States of America

Abstract

To avoid exceeding the Chinook salmon (*Oncorhynchus tshawytscha*) bycatch limit in the North Pacific walleye pollock (*Gadus chalcogrammus*) trawl fisheries, a novel bycatch reduction device design was developed to permit escapement from the trawl before entering the codend (an 'excluder'). An observation made from previous salmon excluder trials is that the escapement rate of salmon was higher for lower towing velocities. In addition, salmonids are known to react to changes in water velocity and tend to orient toward areas of low velocity. Therefore an excluder was designed with the aim of facilitating escapement and attracting salmon to the escape area by generating low flow velocity regions. The flow field in and around the excluder design was analysed using 'Reynolds averaged Navier-Stokes' (RANS) computational fluid dynamics methods. A porous medium approach was used to represent the netting in order to simplify flow simulations. Based on the simulation results, configurations for a 1:2 scale excluder model were selected for testing in a flume tank. Simulation and measurement results showed qualitatively good agreement.

Keywords

Mid-water trawl, salmon bycatch reduction device, computational fluid dynamics, flume tank experiments, species selectivity

Nomenclature

F_i	-	force term, representation for pressure and external forces	[m/s²]
S	-	solidity of netting	[-]
S_i	-	source term	[Pa/m]
c_{drag}	-	dimensionless drag coefficient	[-]
c_{lift}	-	dimensionless lift coefficient	[-]

c_l	-	linear pressure loss coefficient	[kg/(m²s)]
c_q	-	quadratic pressure loss coefficient	[kg/m³]
k	-	dimensionless pressure coefficient	[-]
n_i	-	normal unit vector component of the porous medium	[-]
p	-	pressure	[Pa]
t_{Ai}, t_{Bi}	-	tangential unit vector components of the porous medium	[-]
u_i, u_j	-	velocity component in direction x_i, x_j for $i, j \in [1,2,3]$	[m/s]
x_i, x_j	-	coordinate direction for $i, j \in [1,2,3]$	[m/s]
α_{in}	-	angle of incidence	[°]
γ	-	anisotropy coefficient	[-]
ν	-	kinematic viscosity of the fluid	[m²/s]
σ	-	stress	[N/m²]

Introduction

In the commercial walleye pollock (*Gadus chalcogrammus*) fisheries in the Gulf of Alaska and Bering Sea and Aleutian Islands, bycatch allowance of Chinook salmon (*Oncorhynchus tshawytscha*) is limited and exceeding this amount has the potential to close the pollock fishery every year (Fissel et al. 2016). Given that total annual catch of pollock is over a million metric tons (Ianelli et al. 2013, Witherell & Armstrong 2015), ways to reduce salmon bycatch are urgently sought.

Behavioural differences between salmon and pollock may allow for the implementation of a bycatch reduction device (BRD) in the trawl that allows most of the salmon (bycatch species) to escape while retaining most of the pollock (target species). It was observed that pollock rarely swim forward in the trawl or only do so for short distances, while salmon have been observed actively swimming forward in a towed trawl (Gauvin & Paine 2004). To use this difference in behaviour to increase salmon escapement, a BRD requires an escapement portal that is accessible to salmon swimming in the direction of tow, and that the trawl is towed at a velocity that correlates to the swimming abilities of salmon. Following this approach, several ‘salmon excluder’ designs have been tested with mixed success (Gauvin & Gruver 2008, Gauvin et al. 2011, Gauvin et al. 2013, Gauvin et al. 2015). Notable in the results of these excluder trials is a trend of higher escapement rates with slower towing velocities. Trial tows in the Bering Sea were conducted at speeds of 1.5 to 2.2 m/s and in the Gulf of Alaska at speeds of 1.3 to 1.5 m/s (Gauvin 2016). Given that the cruising speed of adult

salmon is approximately 1.2 m/s (Bell 1991) suggests that the towing speed of the trawl is too fast to achieve desired salmon escapement rates. However, a slower towing speed might result in poor gear performance for catching pollock (Gauvin 2016). Thus, we proposed to increase the efficacy of the excluder by reducing the local flow velocity in the area of the escapement portal while maintaining the towing speed of the trawl to allow for improved salmon escapement with minimal loss of pollock.

In the shrimp trawl fishery it is established practice to facilitate escapement of bycatch species using slack water areas in proximity of escapement portals (Engås et al. 1999, Eayrs 2007, Cha et al. 2011, Parsons et al 2012). However, catch per haul in the shrimp fishery is in the order of 100 kilograms (He et al. 2007); whereas, the catch per haul in the pollock fishery is in the order of 100 metric tons (Gauvin & Paine 2004). Given this difference in scale, a transferable mechanism to generate slack water in and around an escape portal is not readily available for the pollock fishery.

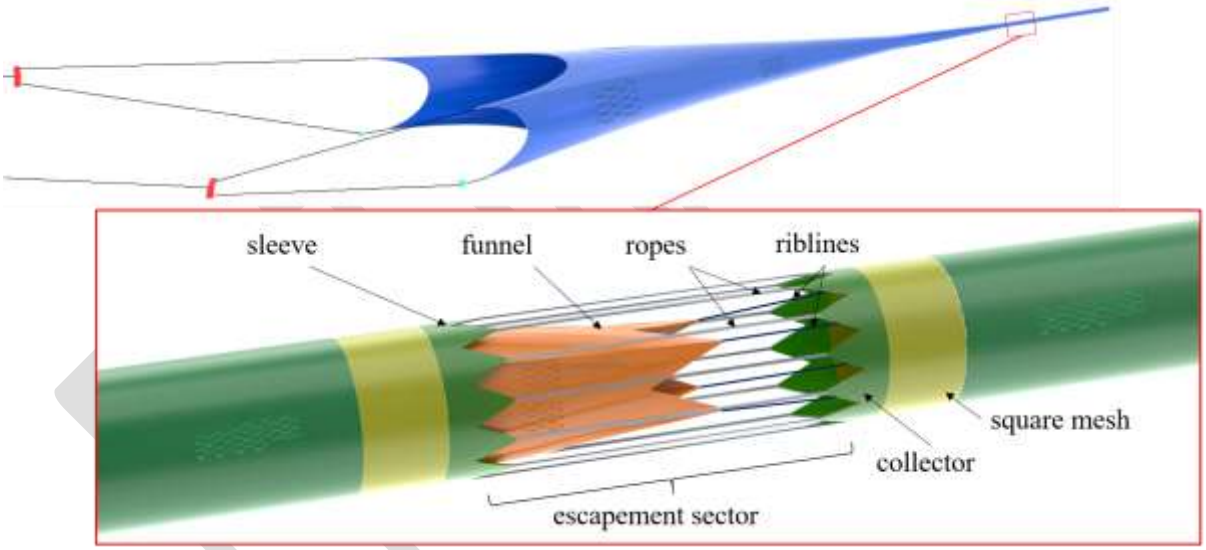

Figure 1
Initial salmon excluder concept, highlighting key elements of the design and intended placement in the trawl.

A new salmon excluder concept was proposed by authors Yochum and Stone for the North Pacific walleye pollock fishery. It consists of a net funnel, an escapement sector, and a kite-spread collector area (Figure 1). The forward section of the excluder and the collector are connected via ropes that encircle the funnel and escapement sector. The two sections are also connected by way of the four riblines that extend through the entirety of the trawl, including through the funnel. The load introduction in the front part of the excluder section is realized via

a sleeve at the start of the funnel. The funnel and sleeve are designed to create a wake region (i.e., low flow) in the escapement sector, which should facilitate (and permit) the salmon to escape out of the trawl.

The choice of netting material for a given funnel geometry is critical to generate the desired change in water velocity in the escapement area, while also preventing reduced flow and, therefore, catch accumulation in front of the funnel. Consequently, flow simulations with Reynolds-averaged Navier-Stokes (RANS) methods were completed to investigate the flow field in and around the excluder using different netting types for the funnel (i.e., twine and mesh size) and configurations. A porous medium approach was used to simplify the netting in the flow simulation, and the netting was assumed to be rigid.

An experiment with a 1:2 scale excluder model was carried out in a flume tank. Measurement of flow during the experiment allowed verification and description of the intended areas of low flow in the excluder model, and a numerical simulation of the flow was compared to the measurements to assess reliability of the simulation.

Methods

Porous Medium Approach

RANS methods are widely used and well documented for solving engineering flow problems (e.g., Pope 2009 or Ferziger & Peric 2002). However, RANS flow simulations of nets and trawls require simplifications. The computational cost to resolve every mesh of the netting is too high to solve using existing computers or clusters. A practical approach was proposed by Patursson et al. 2010. For this approach, the meshes of the netting are not resolved; instead a 'porous medium' is implemented that replicates the hydrodynamic properties the netting exerts on the fluid. According to Taylor & Batchelor 1949, the hydrodynamic properties to be identified are a pressure loss over the netting and a flow deflection induced by the netting. Following Schubauer et al. 1950, the flow deflection may be described by a tangential stress.

For the implementation of a porous medium, the incompressible Navier-Stokes equation (summation notation) is extended by a source term S_i

$$\frac{\partial u_i}{\partial t} + \frac{\partial (u_i u_j)}{\partial x_j} = F_i + \nu \frac{\partial^2 u_i}{\partial x_j^2} + \frac{1}{\rho} S_i, \quad i, j \in [1,2,3], \tag{1}$$

where $u_i(x_i,t), u_j(x_j,t)$ for $i, j \in [1,2,3]$ denote the velocity components and x_i, x_j for $i, j \in [1,2,3]$ denote the directions of the coordinates. In F_i the external force

and pressure forces are grouped together. The source term S_i represents a stress (or pressure) σ_i per distance and has to be determined for every direction x_i.

The porous medium approach was adapted by various scientists (Breddermann 2011, Zhao et al. 2013, Bi et al. 2014, Breddermann 2015, Breddermann 2017) for flexible marine structures like aquaculture sea-cages and plankton nets. Differences in the approaches pertain to how the hydrodynamic properties of the netting are taken into account and limitations in the application to complex geometries.

Patursson et al. 2010 and Zhao et al. 2013 used experimental data to determine the source term. However, their approaches were limited to cases where the angle between incident flow direction and net panel or object was known in advance. Bi et al. 2014 enhanced the above mentioned approaches and introduced a transformation matrix to allow for more complex shaped geometries with net panels oriented at arbitrary positions. This transformation is applied between a global coordinate axis and the normal vector of the net panel. This gives only an estimate of the true angle of attack of the net panel, which creates inherent error in the source term.

Breddermann 2017 presented a transformation that takes into account incident flow direction and net panel orientation. Computation of the flow requires the source terms to be in a global coordinate system that is associated to the flow solver with the directions ${}^{global}x_i$. However, the hydrodynamic properties of a net panel (e.g., pressure loss over the panel and flow deflection or lift and drag coefficient of the panel) are given in a local coordinate system aligned to the net panel, Figure 2.

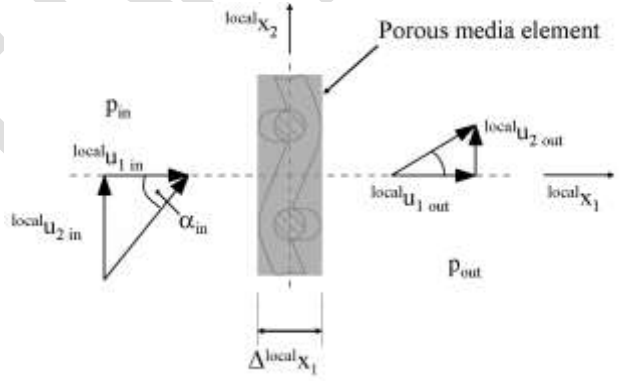

Figure 2
Local coordinate system aligned to the net panel [Breddermann 2017].

Thus, the local source term ${}^{local}S_i$ may be considered known,

$$ {}^{local}S_i = \frac{{}^{local}\sigma_i}{\Delta^{local}x_1}, \tag{2} $$

where $\Delta^{local}x_i$ is given by the thickness of the porous medium. The local stress ${}^{local}\sigma_1$ in the normal direction of the net panel is the pressure loss over the panel and may be expressed by

$$ {}^{local}\sigma_1 = -\Delta p = -c_l \cdot {}^{local}u_1 - c_q \cdot \left|{}^{local}u_1\right| \cdot {}^{local}u_1 = -\frac{\rho \cdot \left|{}^{local}u_1\right| \cdot {}^{local}u_1 \cdot k}{2}, \tag{3} $$

where k is a dimensionless pressure loss coefficient, c_l is a linear pressure loss coefficient, and c_q is a quadratic pressure loss coefficient. The stresses in the tangential direction may be expressed according to Vaisman & Gol'dshtik 1978

$$ {}^{local}\sigma_{2,3} = -\rho \cdot \left|{}^{local}u_1\right| \cdot {}^{local}u_{2,3} \cdot \left(1 - \frac{1}{\exp\left(k \cdot (1-S)^2 \cdot \gamma\right)}\right), \tag{4} $$

where S denotes the solidity of the netting and γ is an anisotropy coefficient. Deducing k and γ from given lift and drag coefficients from netting is uncomplicated. Also, the expression proposed for ${}^{local}\sigma_i$ may change as required to fit data at hand for netting material.

As can be noted from Equations 3 and 4 for the calculation of the local source terms, the local velocities are required. Because the fluid solver provides the velocities in its global coordinate system, a further transformation is necessary. Switching to vector notation,

$$ {}^{global}\underline{S} = \begin{bmatrix} {}^{global}S_1 \\ {}^{global}S_2 \\ {}^{global}S_3 \end{bmatrix}, \tag{5} $$

the necessary transformations are expressed as follows:

$$ {}^{local}\underline{u} = {}^{local\,global}\underline{\underline{T}} \cdot {}^{global}\underline{u}, \tag{6} $$

$$ {}^{global}\underline{S} = {}^{global\,local}\underline{\underline{T}} \cdot {}^{local}\underline{S}. \tag{7} $$

$\underline{\underline{T}}$ denotes the transformation matrix for which

$$ {}^{local\,global}\underline{\underline{T}} = {}^{global\,local}\underline{\underline{T}}^T. \tag{8} $$

holds true and is given by

$$ {}^{globallocal}\underline{\underline{T}} = \begin{bmatrix} n_1 & t_{A1} & t_{B1} \\ n_2 & t_{A2} & t_{B2} \\ n_3 & t_{A3} & t_{B3} \end{bmatrix}. \tag{9} $$

The components of the normal unit vector of the netting panel are denoted by n_i, and t_{Ai} and t_{Bi} denote the components of the unit vectors tangential. The normal unit vector and its components are usually provided by the fluid solver. The first tangential unit vector may be chosen from the following

$$ \underline{t}_A := \frac{1}{|\underline{t}_A|}\begin{bmatrix} -n_2 \\ n_1 \\ 0 \end{bmatrix}, \quad \underline{t}_A := \frac{1}{|\underline{t}_A|}\begin{bmatrix} -n_3 \\ 0 \\ n_1 \end{bmatrix}, \quad or\ \underline{t}_A := \frac{1}{|\underline{t}_A|}\begin{bmatrix} 0 \\ -n_3 \\ n_2 \end{bmatrix}. \tag{10} $$

The second tangential unit vector is constructed by a rotation of the first tangential vector by $\pi/2$

$$ \underline{t}_B = \underline{\underline{R}} \cdot \underline{t}_A. \tag{11} $$

For the rotation of $\pi/2$, the rotation matrix $\underline{\underline{R}}$ is given by

$$ \underline{\underline{R}} = \begin{bmatrix} n_1^2 & n_1 n_2 - n_3 & n_1 n_3 + n_2 \\ n_2 n_1 + n_3 & n_2^2 & n_2 n_3 - n_1 \\ n_3 n_1 - n_2 & n_2 n_3 + n_1 & n_3^2 \end{bmatrix} \tag{12} $$

and it follows for $\underline{t}_B$

$$ \underline{t}_B = \begin{bmatrix} n_1^2 \cdot t_{A1} + (n_1 n_2 - n_3) \cdot t_{A2} + (n_1 n_3 + n_2) \cdot t_{A3} \\ (n_2 n_1 + n_3) \cdot t_{A1} + n_2^2 \cdot t_{A2} + (n_2 n_3 - n_1) \cdot t_{A3} \\ (n_3 n_1 - n_2) \cdot t_{A1} + (n_2 n_3 + n_1) \cdot t_{A2} + n_3^2 \cdot t_{A3} \end{bmatrix}. \tag{13} $$

At this point all necessary components of the transformation matrices are identified. The fluid solver used for this study was ANSYS CFX and the above equations have been implemented in a "CFX Expression language (CEL)" routine.

Table 1
Domain specifications.

Type	Geometry modelled	Domain shape	Domain size (length x extent)	No. of grid elements
			[m]	$x10^6$
1:1 scale excluder	quarter	quarter of cylinder	100 x radius 25	7.6
1:2 scale flume tank configuration	half	cuboid	50 x 4 x 4	12.3

Table 2
Netting specifications.

Section of device	Stretched mesh size	Solidity	γ	c_q	c_l
	[mm]			[kg/m³]	[kg/(m²s)]
1:1 scale excluder, funnel, Ultracross netting,	44.5	0.31	0.51	51.95	451.61
1:1 scale excluder, funnel, Eurocross netting	52	0.27	0.46	41.54	350.48
1:1 scale excluder, funnel, Ultracross netting	75	0.50	1	97.97	919.33
1:1 scale excluder netting	100	0.39	0.59	63.07	565.24
1:2 flume tank configuration, forward section and funnel	100	0.32	0.52	52.28	454.92
1:2 flume tank configuration, sleeve, collector, intermediate section between excluder and codend	100	0.20	0.41	26.13	215.75

Computational Set Up
Two computational domains were set up for this study. One was based on a preliminary net plan of the excluder in 1:1 scale. The number of meshes were converted to dimensions assuming a constant hanging ratio of 0.3. The simulations served to assess the excluder design in general and to determine the effect of different funnel nettings on the flow field. Flow simulations were conducted prior to the experiments in the flume tank. The second set up was modelled to replicate the 1:2 scale configuration that was tested in the flume tank and thus served for validation purposes. The netting material was assumed to be rigid; changes in the netting geometry due to fluid loads were not considered. The domains as

well as the boundary conditions are depicted in Figure 3. The domain specifications are given in Table 1. Specifications of the netting are given in Table 2. The pressure loss coefficient k (c_l and c_q, respectively, Eq. 3) and the anisotropy coefficient γ for the nettings were deduced by the expression for lift and drag given in Løland 1991:

$$c_{drag} = 0.04 + \left(-0.04 + S - 1.24 \cdot S^2 + 13.7 \cdot S^3\right) \cdot \cos \alpha_{in}, \tag{14}$$

$$c_{lift} = \left(0.57 \cdot S - 3.54 \cdot S^2 + 10.1 \cdot S^3\right) \cdot \sin 2\alpha_{in}. \tag{15}$$

In the simulations fresh water was selected as the fluid. The inlet fluid velocity for the 1:1 scale excluder section was 1.8 m/s and 0.91 m/s for the 1:2 scale flume tank configuration.

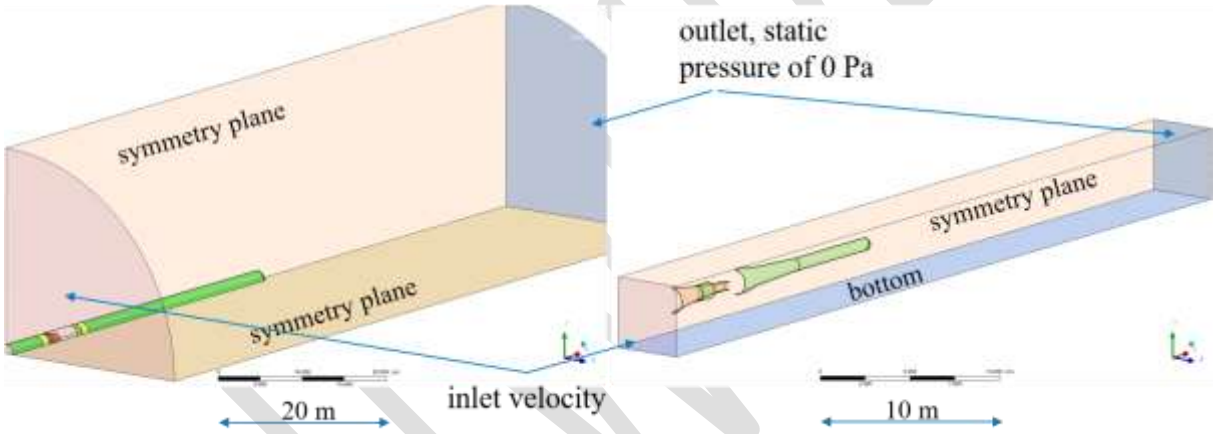

Figure 3
Computational domains. On the left side the 1:1 scale excluder section is depicted. Not marked is the opening boundary condition. On the right the 1:2 scale flume tank setup is depicted. Not shown are the side (wall boundary condition) and the top (opening boundary condition).

Flume Tank Experiments
Experiments were conducted in the flume tank of the Fisheries and Marine Institute of Memorial University (Winger et al. 2006) in March 2019 to test the salmon excluder design (Figure 4). The flow velocity was approximately 0.91 m/s. Velocity readings were taken at several transects in the excluder section with a Valeport Electromagnetic Current Flow Sensor (Model 802, 3.2 cm discus) mounted at an hand-held probe support.

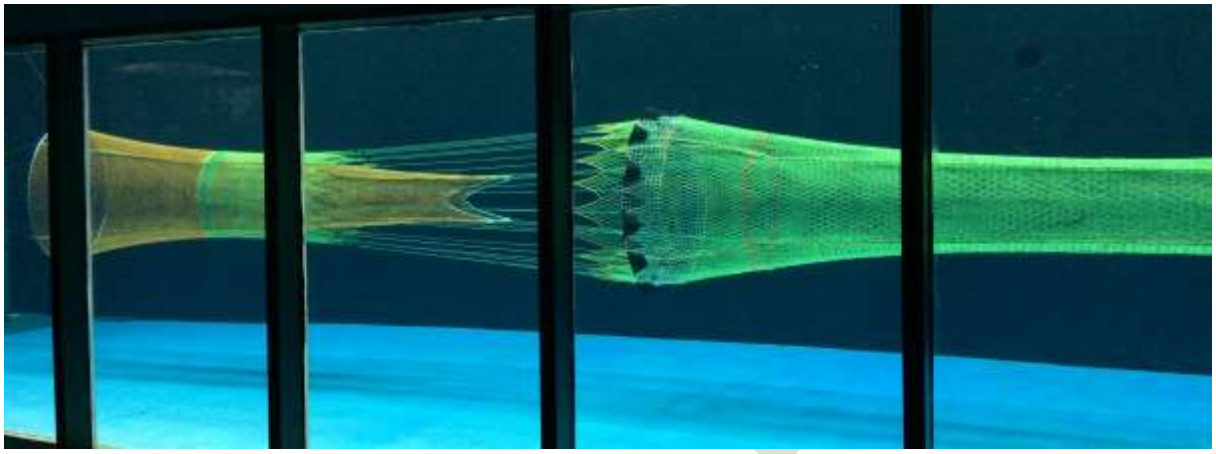

Figure 4
1:2 scale excluder in the flume tank.

Results

To evaluate the effect of different funnel netting, velocity information was sampled at three transects depicted in Figure 5: in front of the funnel in the netting tube, at the funnel entrance and at the funnel exit. The velocity data was normalized by the undisturbed inlet velocity and is given in Figure 6. Figure 7 provides a comparison of the results from the simulation and flume tank experiments. The velocity data is normalized by the flume tank velocity.

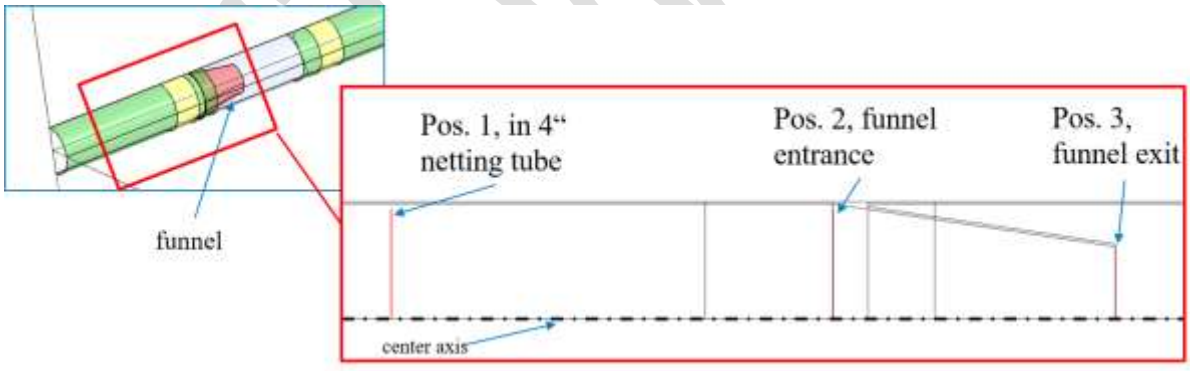

Figure 5
Sampling positions to collect water velocity data within the excluder.

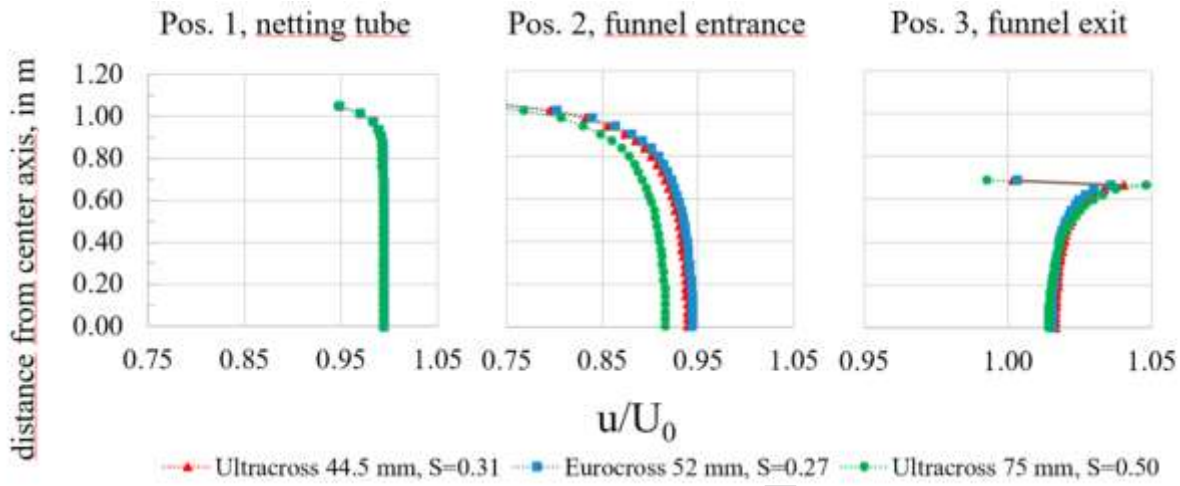

Figure 6
Velocity profiles at positions depicted in Figure 5.

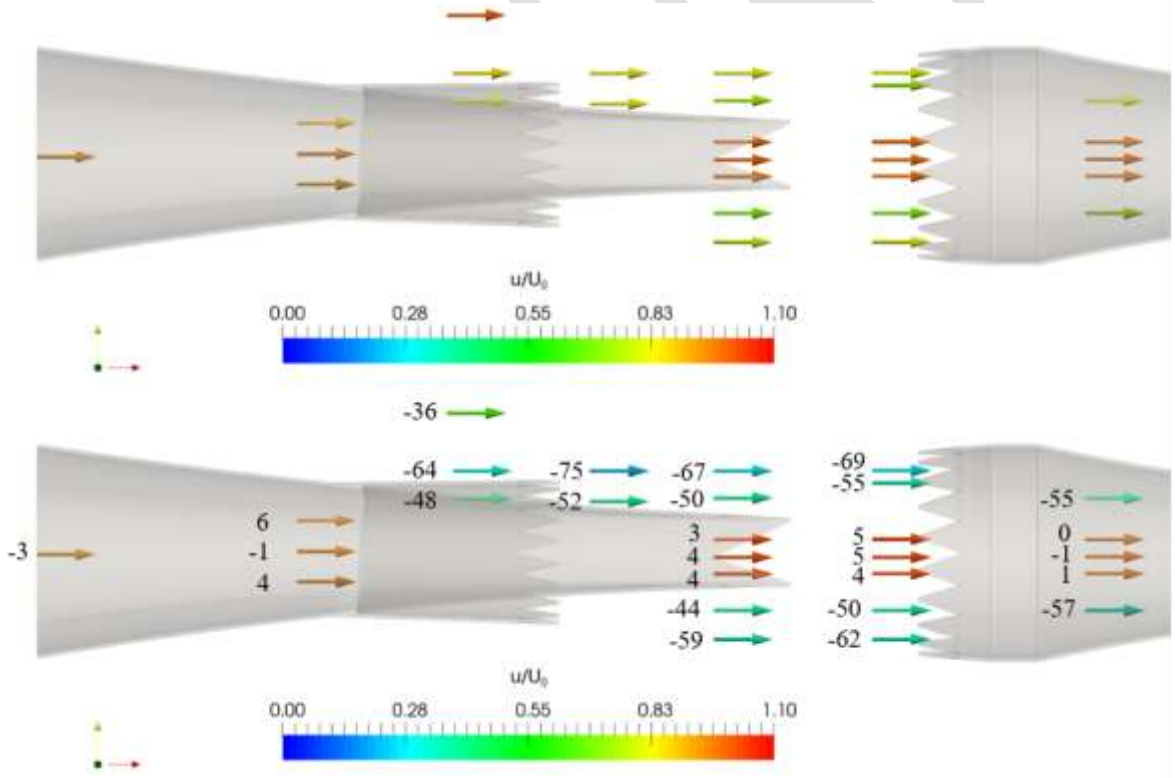

Figure 7
Starting points of arrows mark the sampling positions. Top: Velocity readings of the flume tank experiment normalized by the flume tank velocity. Bottom: Results of the CFD simulation normalized by the inlet velocity. Numbers denote the deviation in percent to the flume tank experiments. Negative values indicate a slower velocity in the simulation result.

Discussion

Fluid simulation and flume tank experiments showed that the proposed salmon excluder concept is successful from a hydrodynamic point of view. The desired wake region develops around the funnel, where salmon escapement is intended, and the flow field at the funnel entrance is not slowed down considerably. The graphs in Figure 6 indicate that there is no major difference in the flow field of the Eurocross and Ultracross netting options that were simulated with the solidities of approximately 0.3. According to the formulation of Løland (Eqs. 14 and 15), it is the solidity which governs the hydrodynamic properties. Thus, differences are not expected. The use of the Ultracross netting with a solidity of 0.5 results in a more pronounced deceleration of the flow at the funnel entrance, which may increase the likelihood of catch accumulation in front of the funnel. At the funnel exit, the flow fields are similar again and accelerated in comparison to the undisturbed flow velocity.

Comparing the wake region around the funnel in Figure 7, the flow simulation overestimates the change in water flow in the desired wake region (i.e., predicts slower water than was observed in the flume tank). Because the flow velocity in the center is in good agreement with the measurement, we conclude that the flow rate in and out of the funnel and through the funnel netting is predicted reasonably. However, since the extent of the wake region is overestimated, it seems that the flow through the netting is deflected more than predicted. Hence, it is assumed, that the anisotropy coefficient γ, which will affect the flow deflection, is not well captured. Furthermore, it is assumed that the opening of the meshes and hence, the solidity, is fixed for the complete net. This simplification might not be reasonable because the opening of the meshes might differ considerably according to the loads acting on the mesh. Since the opening of the meshes governs the solidity and in succession the hydrodynamic properties, it is of importance to develop the presented porous medium approach further and include the solidity as a local variable.

Conclusion

Computational fluid simulations showed qualitatively good agreement with measured data collected in the flume tank. These results will help chose appropriate netting prior to the construction of the excluder for full scale trials or model tests. However, quantitatively the measurement and simulation results differed noticeably. To capture the flow deflection more accurately, experiments to determine lift and drag of net panels are necessary. These data will help validating if the formulations used are applicable to the netting investigated.

A future task should be the further development of the porous medium approach. Extending it by a local solidity, the fluid solver and a structural solver can be coupled, where the structural solver predicts shape and solidity based on a simulated flow field. Processing the structural and the fluid solver in a loop will result in a more realistic approximation of the investigated net and flow field.

Disclaimer: The scientific results and conclusions, as well as any views or opinions expressed herein, are those of the author(s) and do not necessarily reflect those of NOAA or the Department of Commerce.

References

1. Bell, M. C. – Fisheries handbook of engineering requirements and biological criteria – U.S. Army Corps of Engineers, Third edition, 1991, 341 pp., https://apps.dtic.mil/dtic/tr/fulltext/u2/a275026.pdf
2. Bi, C.-W., Zhao, Y.-P., Dong, G.-H., Zheng, Y.-N., and Gui, F.-K. – A numerical analysis on the hydrodynamic characteristics of net cages using coupled fluid–structure interaction model – Aquacultural Engineering, 59, 2014, p. 1–12
3. Breddermann, K., Paschen, M. – On the way to plankton net calibration – Contributions on the Theory of Fishing Gears and Related Systems, 7 (Proceedings of the DEMaT 2011), 2011, ISBN 978-3-8440-0468-7, pp. 153-167
4. Breddermann, K. – Methoden zur Simulation von Strömungen um und durch Aquakulturanlagen mit RANSE-Verfahren (*Methods to simulate the flow through and around aquaculture cage systems with RANS solver*) – Rostocker Meerestechnische Reihe (Hrsg. M. Paschen): Beiträge zur Theorie und zum Entwerfen von Netzkäfigen für die Offshore-Aquakultur, 2015, ISBN 978-3-8440-4181-1, pp. 49-71
5. Breddermann, K. – Filtration Performance of Plankton Nets used to catch Micro- and Mesozooplankton – Ph.D. thesis, Rostocker Meerestechnische Reihe (Hrsg. M. Paschen), 2017, ISBN 978-3-8440-5405-7
6. Engås, A., Foster, D., Hataway, B. D., Watson, J. W., and Workman, I. – The behavioral response of juvenile red snapper (*Lutjanus campechanus*) to shrimp trawls that utilize water flow modifications to induce escapement – Marine Technology Society Journal, 33(2), pp. 43-50
7. Ferziger, J. and Peric, M. – Computational Methods for Fluid Dynamics – Springer-Verlag, third printing, 2002, ISBN 978-3-642-56026-2
8. Fissel, B., Dalton, M., Felthoven, R., Garber-Yonts, B., Haynie, A., Kasperski, S., Lee, J., Lew, D., Santos, A., Seung, C., and Sparks, K. – Stock assessment and fishery evaluation report for the groundfish fisheries of the Gulf of Alaska and Bering Sea/Aleutian Islands area: economic status of the groundfish fisheries off Alaska – Unpublished Report, National Marine Fisheries Service, Seattle, Wash., https://www.afsc.noaa.gov/REFM/Docs/2016/economic.pdf
9. Gauvin, J. R., and B. Paine. – EFP 03-01: test of a salmon excluder device for the pollock trawl fishery January 2003 through March 2004 – NOAA EFP Final Report, 2004, p. 24
10. Gauvin, J., and Gruver, J. – Final report on EFP 05-02 to develop a workable salmon excluder device for the Bering Sea pollock fishery – NOAA EFP Final Report, 2008, p. 15

11. Gauvin, J., Gruver, J. and Rose, C. – Final report for EFP 08-02 to explore the potential for flapper-style salmon excluders for the Bering Sea pollock fishery – NOAA EFP Final Report, 2011, p. 23

12. Gauvin, J., Gruver, J., McGauley, K., and Rose, C. – Salmon excluder EFP 11-01 – NOAA EFP Final Report, 2013, p. 43

13. Gauvin, J., Gruver, J. and McGauley, K. – Central Gulf of Alaska salmon excluder EFP 13-01 –NOAA EFP Final Report, 2015, p. 29

14. Gauvin, J. – Bering Sea salmon excluder EFP 15-01 – NOAA EFP Final Report, 2016, p. 25

15. He, P., Goethel, D. and Smith, T. – Design and test of a topless shrimp trawl to reduce pelagic fish bycatch in the Gulf of Maine pink shrimp fishery – Journal of Northwest Atlantic Fisheries Science, vol. 38, 2007, pp. 13-21

16. Ianelli, J. N., Honkalehto, T., Barbeaux, S., Kotwicki, S., Aydin, K., and Williamson, N.– Assessment of the walleye pollock stock in the Eastern Bering Sea. In Stock assessment and fishery evaluation report for the groundfish resources of the Bering Sea/ Aleutian Islands regions for 2014 – North Pacific Fishery Management Council, Anchorage, AK, 2014, pp. 51-56

17. Løland, G. – Current force on and flow through fish farms – Dr. Eng. Dissertation. Division of Marine Hydrodynamics, Norwegian Institute of Technology, 1991, ISBN 82-7119-269-8

18. Patursson, O., Swift, M. R., Tsukrov, I., Simonsen, K., Baldwin, K., Fredriksson, D. W., Celikkol, B. – Development of a porous media model with application to flow through and around a net panel – Journal of Ocean Engineering, 2010, 37(2), 314–324

19. Pope, S. B. – Turbulent Flows – Cambridge University Press, sixth printing, 2009, ISBN 978-0-521-59886-6

20. Schubauer, G. B. - Aerodynamic characteristics of damping screens - NACA Technical Note 2001, 1950

21. Taylor, G. I. and Batchelor, G. K. – The effect of a wire gauze on small disturbance in a uniform stream – Quarterly Journal of Mechanical and Applied Mathematics, 2, 1949, p. 1-29

22. Vaisman, A. M. and Gol'dshtik, M. A. – Flow through a thin porous layer (grid) – Fluid Dynamics, 1978, p. 545-550

23. Witherell, D., and Armstrong, J. – North Pacific Fishery Management Council groundfish species profiles 2015 – North Pacific Fishery Management Council, 605 West 4th, Suite 306, Anchorage, Alaska 99501-2252

24. Winger, P.D., DeLouche, H., and Legge, G. – Designing and testing new fishing gears: the value of a flume tank - Marine Technology Society Journal, 40, 2006, p. 44-49.

25. Zhao, Y.-P., Bi, C.-W., Dong, G.-H., Gui, F.-K., Cui, Y., and Xu, T.-J. – Numerical simulation of the flow field inside and around gravity cages – Aquacultural engineering, 52, 2013, p. 1–13